Research Square

Preprints are preliminary reports that have not undergone peer review.
They should not be considered conclusive, used to inform clinical practice,
or referenced by the media as validated information.

Eco-Friendly Corrosion Inhibitor Derived from Acacia nilotica Fruit Extract for Mild Steel Protection in Acidic Media

Gulshan Kumar Thakur
Shri Shankaracharaya Professional University
Monika Das
Shri Shankaracharaya Professional University
Bhawana Jain
Siddhachalam Laboratory
Prachi P Nimje
prachinimje56@gmail.com

Shri Shankaracharaya Professional University
Akhil Saxena
Chandigarh University

Research Article

Keywords: Mild steel, Green corrosion inhibitor, Adsorption, Electrochemical analysis, Surface analysis

Posted Date: August 27th, 2026

DOI: https://doi.org/10.21203/rs.3.rs-10510365/v1

License: This work is licensed under a Creative Commons Attribution 4.0 International License.
Read Full License

Additional Declarations: No competing interests reported.

Eco-Friendly Corrosion Inhibitor Derived from *Acacia nilotica* Fruit Extract for Mild Steel Protection in Acidic Media

Gulshan Kumar Thakur[1], Monika Das[1], Bhawana Jain[2], Prachi P Nimje[1*], Akhil Saxena[3]

[1]Department of Chemistry, Shri Shankaracharaya Professional University, Bhilai, Chhattisgarh, 490020 India.

Email: gulshan04101987@gmail.com

Email: cool.monika11988@gmail.com

[2]Department of Chemical Sciences, Siddhachalam Laboratory, Raipur, Chhattisgarh, 493221 India.

Email: bhawanajain123@gmail.com

[3]Department of Chemistry, Chandigarh University, Mohali, Punjab, 140413, India.

Email: akhil.uis@cumail.in

*Corresponding Author

Prachi P Nimje[1*]

Email: prachinimje56@gmail.com

Abstract

In this work, the corrosion-inhibiting properties of *Acacia nilotica* fruit extract (ANFE) on mild steel in 1 M HCl were investigated. To evaluate the corrosion-inhibiting efficacy of ANFE, weight loss measurements and electrochemical techniques including Potentiodynamic Polarization (PDP) and Electrochemical Impedance Spectroscopy (EIS) were employed. For the ANFE inhibitor, the maximum corrosion inhibition efficiency was achieved at an optimal concentration of 20 ppm of crude extract of ANFE. PDP studies revealed that the inhibitors exhibited mixed-type behavior, albeit predominantly cathodic in nature. According to EIS studies, a maximum corrosion inhibition efficiency of 94.47% was observed at the optimal inhibitor concentration. Electrochemical studies indicated that the inhibitor significantly increased the charge transfer resistance while simultaneously reducing the corrosion current density. The adsorption process was elucidated using the Langmuir adsorption isotherm. The mixed-mode interaction between the inhibitor and the metal surface was evidenced by the changes in the activation energy values observed upon the addition of the inhibitor. The adsorption of ANFE molecules onto the metal surface and the consequent corrosion protection was further confirmed through surface characterization techniques, such as Scanning Electron Microscopy coupled with Energy-Dispersive Spectroscopy.

Keywords: Mild steel; Green corrosion inhibitor; Adsorption; Electrochemical analysis; Surface analysis.

1. Introduction

Mild steel is one of the most widely utilized materials in engineering, owing to its low cost, excellent mechanical properties, and ready availability. However, its application in long-term operations within the construction, petrochemical, oil, and chemical industries faces a significant impediment: its rapid corrosion in challenging environments, such as those involving acidic or saline conditions [1-3]. It is imperative to develop effective methods for corrosion prevention, as material degradation due to corrosion can pose serious safety and economic risks. The use of plant mediated corrosion inhibitors has been identified as one of the most effective, economical, and efficient strategies for preventing corrosion due to presence of vast majority of phytoconstituents such as alkaloids, flavonoids, terpenes, carbohydrates, polyphenols and cholesterol etc. [4, 5]. To minimize direct contact between the metal and the corrosive environment, phytoconstituent's of plants typically function by adsorbing onto the metal surface and forming a protective layer. Due to the presence of lone pairs of electrons and π-electron systems which facilitate strong bonding with the metal surface it has been observed that phytoconstituent's of inhibitor molecules containing heteroatoms such as nitrogen, phosphorus, oxygen, and sulfur possess superior corrosion-inhibiting capabilities. Phytoconstituent's containing multiple heteroatoms are increasingly attracting the attention of researchers due to their extensive surface coverage and high adsorption propensity. These molecules readily adsorb onto the surface of mild steel through physical and chemical adsorption processes, forming a robust protective layer that acts as a powerful barrier against corrosive elements [6-9].

In this study, a highly effective corrosion inhibitor i.e. ANFE for mild steel in a corrosive environment has been investigated. Heteroatom containing phytoconstituent's significantly enhance the adsorption properties of the ANFE onto the mild steel surface; this factor is responsible for its exceptional inhibitory performance. The overall corrosion rate is reduced through the effective suppression of cathodic reactions and anodic metal dissolution, resulting from the formation of a stable and coherent protective layer. Electrochemical investigations, Scanning Electron Microscope (SEM) studies, and weight loss measurements all have confirmed the exceptional inhibitory potential of the ANFE. While electrochemical measurements reveal an increase in charge transfer resistance and a decrease in corrosion current density, weight-loss studies demonstrate a significant reduction in the corrosion rate in the presence of the inhibitor

molecules. Furthermore, SEM analysis has confirmed that, in contrast to the damaged surface observed in the inhibitor-free medium, the metal surface in inhibitor-containing systems was found to be smooth and intact [10].

The results of this investigation indicate that the ANFE holds immense promise for inhibiting the corrosion of mild steel and possesses vast potential for industrial applications. Owing to its strong adsorption characteristics, high inhibitory efficiency, and effective surface protection, the ANFE serves as an effective option for corrosion management in aggressive environments.

2. Materials and methods

2.1 Preparation of Mild Steel Specimens for Weight Loss Measurements

Mild Steel (MS) specimens with known measuring were utilized for weight-loss analysis. Prior to each experiment, the MS specimens were polished to ensure their surfaces were clean and smooth. Emery papers of various grades (400, 600, 800, 1000, and 1200 grit), along with Silicon Carbide (SiC), were employed to clean and level the surfaces of the mild steel specimens. Following the polishing process, all specimens were rinsed with distilled water to remove any impurities accumulated on the surface. Subsequently, the specimens were rinsed with distilled water and then degreased using acetone to eliminate any surface impurities, such as oil or grease. Before being utilized, the specimens were finally dried with hot air and stored in a desiccator to protect them from corrosion caused by atmospheric components [5].

The corrosion inhibition efficiency of ANFE on mild steel was investigated using the weight-loss (gravimetric) method over a temperature range of 298 *K* to 328 *K* and at inhibitor concentrations ranging from 10 to 40 ppm. Each dried specimen was weighed precisely using an analytical balance, and the initial weight (W_1) was recorded in preparation for the weight-loss measurements. Subsequently, the specimens were immersed in the test solution for six hours both with and without the inhibitor at temperatures ranging between 298 *K* and 328 *K*. To determine the final weight (W_2), the specimens were retrieved upon the completion of the immersion period, rinsed with distilled water, carefully cleaned to remove corrosion products, washed with acetone, dried, and re-weighed.

The difference between the initial and final weights was used to calculate the weight loss. equation (1) was used to calculate the corrosion rate (ρ) [1, 3].

$$\rho = \frac{\Delta W}{A\mathrm{t}} \tag{1}$$

Where, A is the metal surface area in cm^2, t is the immersion time (6 h), and ΔW is the weight loss in mg/cm^2 h.

Similarly; the equation (2) was used to measure the percentage inhibition efficiency ($\%\eta_{WL}$) as follows [3, 6]:

$$\%\eta_{WL} = \left(\frac{\rho^1 - \rho^2}{\rho^1} \right) \times 100 \tag{2}$$

Where, ρ^1 and ρ^2 represents the weight loss of the MS strip in the uninhibited and inhibited 1M HCl solution respectively.

2.2. Collection of plant materials and preparation of extract

Acacia nilotica is a common name of *Vachellia nilotica* also known as babul, gum Arabic tree, Kikar. Scientist Carl Linnaeus was first identifying *Acacia nilotica* in 1753 [6a]. Its species plantarum later registered as genus Acacia by botanist Delile with genus-Vachellia. It is collected from Rajnandgaon district of Chhattisgarh state at the mid-March. 20 gm of fruit power in 100 mL of double distilled water were soaked overnight for the complete extraction of phytoconstituents of extract which is used further.

2.3. Electrochemical measurements

Since, corrosion is an electrochemical process; therefore, electrochemical techniques are essential for investigating the inhibition action of corrosion. Hence, electrochemical measurements have been performed after the gravimetric analysis. Three electrode assemblies were used to conduct EIS measurements and Tafel polarization. Electrochemical measurements were conducted using a PGSTAT204 system (Metrohm Autolab), operated through dedicated NOVA 2.6 software installed on a computer for data recording and analysis [11]. Stainless steel coupons were utilised in the preparation of the working electrode. The stainless-steel coupons were insulated with Araldite, departing an exposed surface area measuring $2cm^2$ for electrochemical testing. To attain a smooth and uniform finish, the exposed surface was polished

using gradually finer grades of abrasive paper, before each measurement. The reference and counter electrode were calomel and platinum respectively utilised in this study.

The corrosion potential and current density graph were calculated by plotting the potential versus logarithmic of current which on plotting gives Tafel slopes. The scan rate for these Tafel curves was 0.001V/s, and the current range was from 100nA to 1mA. There is a defined range of potential ranging from -250mV, 250mV [12-13].

In corrosion analysis, the Tafel slopes represent essential parameters, providing vital insights into the cathodic and anodic kinetics impacting the corrosion phenomenon. Equation (3) [14] has been used to determine the corrosion inhibition efficiency, based on the PDP data:

$$\eta\% = \frac{I_{corr} - I^{\circ}_{corr}}{I_{corr}} \times 100 \qquad (3)$$

where $I^{0}corr$ and $Icorr$ are the current densities of corrosion measured without and with expired drugs, respectively. The frequency ranges from 100 kHz to 0.1 Hz, from ten frequency points per decade and an amplitude of 0.01 V for EIS measurements. The stainless steel is submerged in acidic solution for 45 minutes, prior to each experiment, to achieve a stable open-circuit potential. To evaluate the effectiveness of the inhibition the equation (4) [15] has been used:

$$\% = \frac{R_{ct} - R^{0}_{ct}}{R_{ct}} \times 100 \qquad (4)$$

Charge transfer resistances in the presence and absence of drugs R^{0}_{ct} and R_{ct} respectively, have been measured.

2.4. SEM-EDS Analysis

To evaluate surface morphology such as corrosion pits, cracks, and the development of protective layers formed by inhibitors SEM micrographs were acquired at various magnifications using a ZEISS EVO SEM 18/INCA 250 EDX XMAX scanning electron microscope (equipped with a 20 mm Oxford model detector). To perform elemental analysis and identify the chemical characteristics of the surface, the SEM was utilized in conjunction with Energy Dispersive X-ray Spectroscopy (EDS) instrumentation. To obtain a representative profile of elemental distribution, EDS spectra were acquired from specific regions of the steel surface. The obtained spectra were

analyzed using appropriate software to identify and quantify elements present in corrosion products such as Fe and O as well as C, N, P, and Cl ions originating from the adsorbed ANFE.

Based on the detailed information regarding surface morphology and elemental composition obtained through the combined SEM–EDS analysis, it was possible to clearly confirm the adsorption of the inhibitor and the formation of a protective layer on the mild steel surface within the HCl medium.

2. Result and discussion

3.1. Weight Loss Measurements

3.1.1. Effect of Inhibitor Concentration

Using the WL method, the effect of ANFE inhibitor concentration on the corrosion rate of mild steel in an HCl medium was investigated over a period of 6 hours. A high corrosion rate was observed on the MS sample in the absence of the inhibitor gradually increase as temperature increased, indicating the severity of the environment. Upon the addition of the ANFE inhibitor, the weight loss (WL) decreased, signaling that the corrosion rate had been controlled. Although inhibition efficiency increased, the corrosion rate decreased as the inhibitor concentration rose from 10 to 40 ppm. As the concentration increases, this concentration-dependent behavior indicates that the mild steel surface becomes more effectively covered by ANFE inhibitor molecules. The findings have clearly demonstrated that the concentration of the ANFE inhibitor significantly influences its corrosion-inhibition efficiency; specifically, at 298 *K*, this efficiency reaches 94.58% at the optimal inhibitor concentration [Table 1]. At lower inhibitor concentrations, surface coverage is moderate, whereas at higher concentrations, surface coverage becomes nearly complete due to the formation of a protective adsorbed layer of inhibitor molecules. At higher concentrations, the enhanced adsorption of inhibitor molecules is attributed to the interactions occurring between the active sites present on the mild steel surface and the heteroatoms (N, O, and P) of the plant-derived components within the extract [5].

Table 1: Measured parameters for mild steel in 1 M HCl using weight loss, at different concentrations (10–40 ppm) and temperatures (298–328 K), with and without an inhibitor.

Temp.(K) ↓	Corrosion Rate ρ (mg cm^{-2} h^{-1})					Inhibition Efficiency (%*IE*)				
Conc. →	**Blank**	**10**	**20**	**30**	**40**	**Blank**	**10**	**20**	**30**	**40**
298	0.923	0.128	0.107	0.079	0.050	-	86.13	88.40	91.44	**94.58**
308	1.401	0.201	0.189	0.161	0.140	-	85.65	86.50	88.50	90.00
318	3.012	0.497	0.441	0.396	0.365	-	83.49	85.35	86.85	87.88
328	4.326	1.154	1.075	0.878	0.766	-	73.32	75.15	79.70	82.29

3.1.2. Effect of Temperature

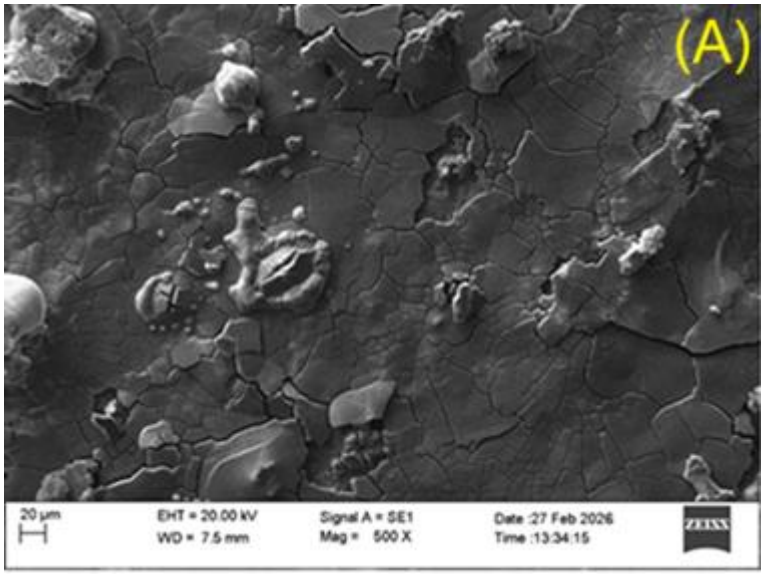
To evaluate the effect of temperature on the inhibition efficiency of ANFE, weight loss measurements were conducted at temperatures ranging from 298 *K* to 328 K. Due to the increased kinetic energy of reactive species and accelerated metal dissolution, the corrosion rate of mild steel in the inhibitor-free HCl solution increased significantly with rising temperature [11]. Even in the presence of the ANFE inhibitor, the corrosion rate increased with temperature; however, at every temperature investigated, this rate remained significantly lower than that observed in the inhibitor-free solution (Table 1). As the temperature increased, the inhibition efficiency decreased slightly, suggesting that the inhibitor molecules undergo partial desorption from the mild steel surface. Although chemical interactions may also play a role in the overall inhibition process, this behavior indicates that the adsorption of ANFE onto the metal surface is predominantly physical in nature [10, 18].

ANFE demonstrated its thermal stability and effectiveness even in an aggressive environment; despite the decline in inhibition efficiency at elevated temperatures, it maintained a remarkable level of inhibition performance even at 328 *K*.

3.2.SEM-EDS analysis

To gain a deeper understanding of the surface protection mechanism, Scanning Electron Microscopy (SEM) was employed to analyze the surface morphology of mild steel samples immersed in a 1 M HCl solution (both with and without the addition of 10–40 ppm of the ANFE

corrosion inhibitor). The SEM microphotographs of the mild steel surface exposed to the HCl solution without the inhibitor clearly revealed roughness, deep corrosion pits, microstructures, and distinct corrosion products. These features indicate localized corrosion attacks and point to the severe corrosion sustained by the metal due to the highly acidic environment. Conversely, the surface morphology of mild steel immersed in an HCl solution containing the ANFE inhibitor showed significant improvement. At the inhibitor concentration of 40 ppm, the steel surface became more uniform and contain minimum roughness, and corrosion defects were almost completely eliminated. The effective adsorption of ANFE inhibitor molecules onto the mild steel surface was confirmed by the formation of a robust and adherent protective layer visible on the inhibited surface. By preventing direct contact between the metal surface and the aggressive HCl medium, this protective layer acts as a physical barrier. The electrochemical and gravimetric results which indicated that corrosion inhibition efficiency increased with increasing inhibitor concentration are strongly corroborated by the SEM observations [3, 25].



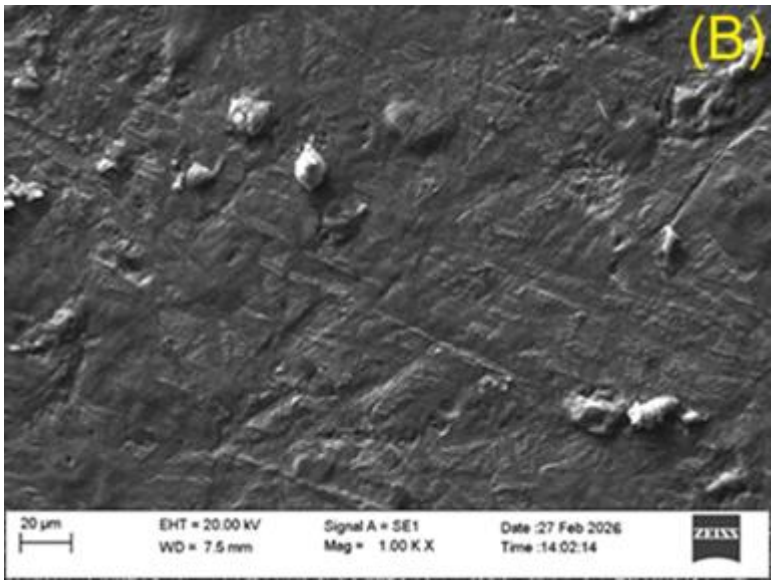


Figure 1. SEM microphotographs for (a) MS in blank solution, and, (b) MS in the presence of ANFE inhibitor solution.

3.3. Energy Dispersive X-ray Spectroscopy (EDS) Analysis

The elemental composition of the mild steel surface was determined, and the adsorption of ANFE in an HCl medium was confirmed using Energy Dispersive X-ray Spectroscopy (EDS). The EDS spectra of the inhibitor-free mild steel sample revealed prominent peaks for iron (Fe) and high intensity for oxygen (O), indicating that iron oxides and hydroxides corrosion products were formed during exposure to the acidic solution [7,9]. When the ANFE inhibitor (200 ppm) was present, a significant reduction in the oxygen signal was observed in the EDS spectrum, signifying a decrease in oxide formation resulting from effective corrosion inhibition. Also table 2 reveled the high amount of aggressive chloride ion (5.56%) without inhibitor molecule responsible to corrode metal surface. While in the presence ANFE inhibitor concentration of chloride ion (0.36%) decreased indicating the protection adsorption of phytoconstituents present in ANFE. The existence of the inhibitor film is further corroborated by the high content of carbon (C) [Table 2]. The identification of these elements provides strong evidence for the adsorption of ANFE inhibitor molecules onto the mild steel surface through heteroatom-metal interactions. Similarly, a reduction in the concentration of chloride ions in the inhibitor-

containing solution indicates the formation of a protective layer on the metal surface, which prevents further attack by chloride ions [9].

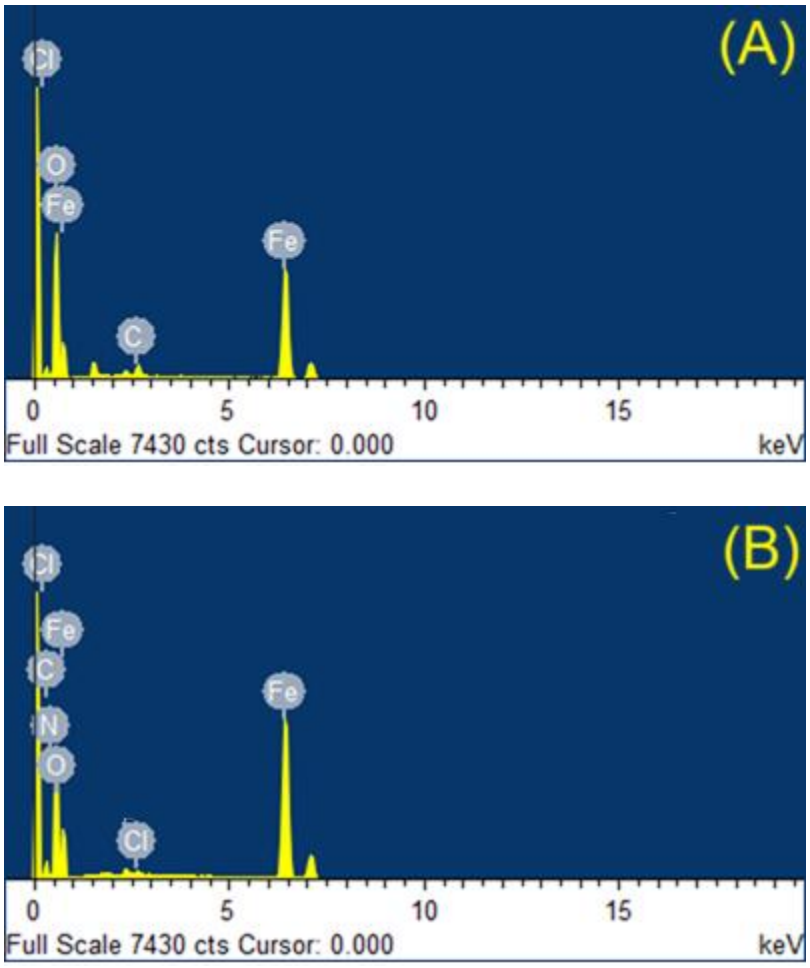


Figure 2. EDS mapping for (a) MS in blank solution, and, (b) MS in the presence of ANFE inhibitor solution.

Table 2: Percentage composition (wt %) of elements for mild steel surface in the absence and presence of inhibitors (80 ppm each) obtained from EDS spectral analysis

Media	**Composition (wt %)**				
	Fe	**Cl**	**O**	**C**	**N**
Mild Steel (MS) in 1 M HCl	92.86	5.56	1.38	0.20	-
MS in 1 M HCl + ANFE	93.23	0.36	0.85	5.52	0.04

3.4. Potentiodynamic Polarization analysis

Corrosion inhibitors diminish corrosion by adsorbing on the metal surface and slowing both anodic and cathodic reactions. Inhibitor performance can be evaluated using the corrosion current density (Icorr), where reduced values suggest greater inhibition efficiency [16]. Figure 1 presents Tafel plots illustrating the polarization behavior of stainless steel with and without expired drugs at different concentrations. Through extrapolation of the polarization curves, numerous Potentiodynamic polarization characteristics data, including corrosion potential (E_{corr}), corrosion current density (I_{corr}), and anodic (βa) and cathodic (βc) Tafel slopes are derived and shown in Table 1. Using Equation (v), the percentage inhibition efficiency (η %) was determined, which is additionally mentioned in Table 2 [17-21].

In the corrosive environment, the cathodic and anodic polarization characteristics of steel has been shown in Figure 1. Inhibitors are categorized as mixed-type, cathodic, and anodic based on the measured E_{corr} values. When the alteration in E_{corr} is less than 85 mV, an inhibitor is called mixed-type. In current study the similar βa and βc and a slight variation in E_{corr} values has been taken then the expired Methotrexate drug performs as a mixed-type inhibitor, effecting both cathodic and anodic process. ANFE successfully reduces the corrosion process which was represented by Tafel lines. These lines stay constant when the inhibitor is present during the corrosion process. In addition, the impact of inhibition increases when the concentration of inhibitor increases [22].

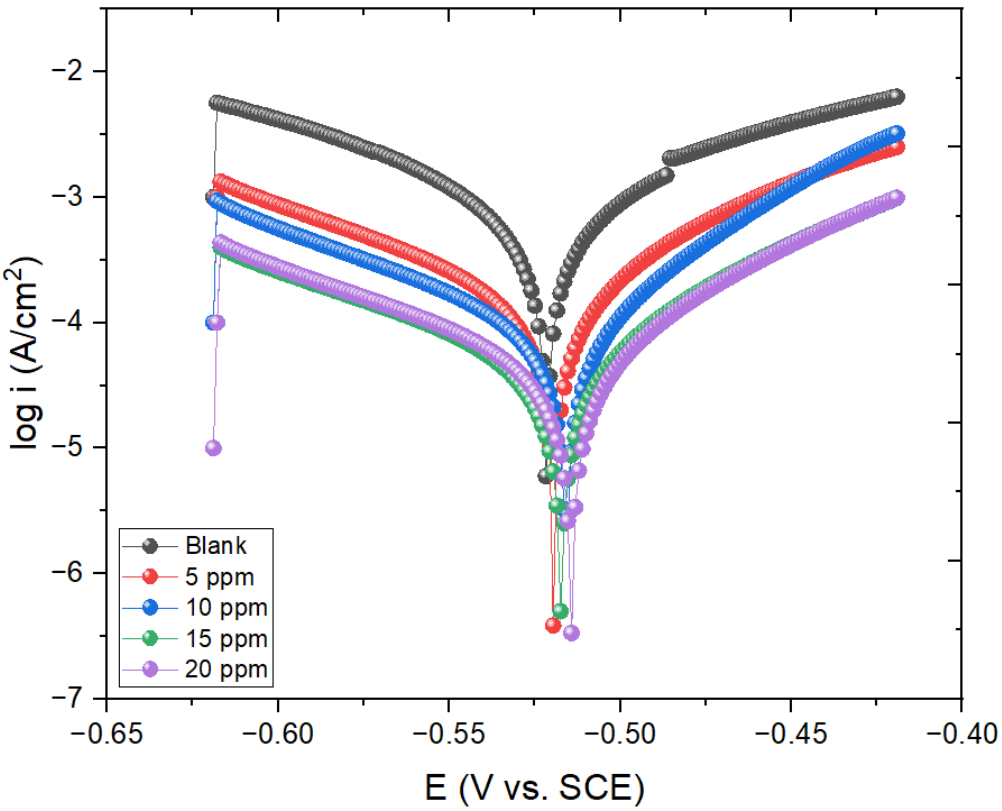


Figure 3: Potentiodynamic polarization curves were recorded in both the absence and presence of different concentrations of ANFE to investigate its effect on corrosion processes.

A considerable reduction in corrosion current density (9.80 x 10^{-5} A/cm^2) and maximum inhibition efficiency was observed at 20 ppm which has been indicated by Table 1. This higher concentration of ANFE decreases the I_{corr} of steel. Also, the high inhibition efficiency and reduction in corrosion current density signifies the adsorption of ANFE onto metal surface restricting corrosion of steel. This also signifies a slow rate of loss of metal which in actuality improves the reliability and durability of stainless steel. These results make it clear that ANFE can work as a competent and ecologically friendly corrosion inhibitor, which gives us both financial and sustainable advantages.

Table 3: PDP parameters at varying concentrations of ANFE in 1 M HCl.

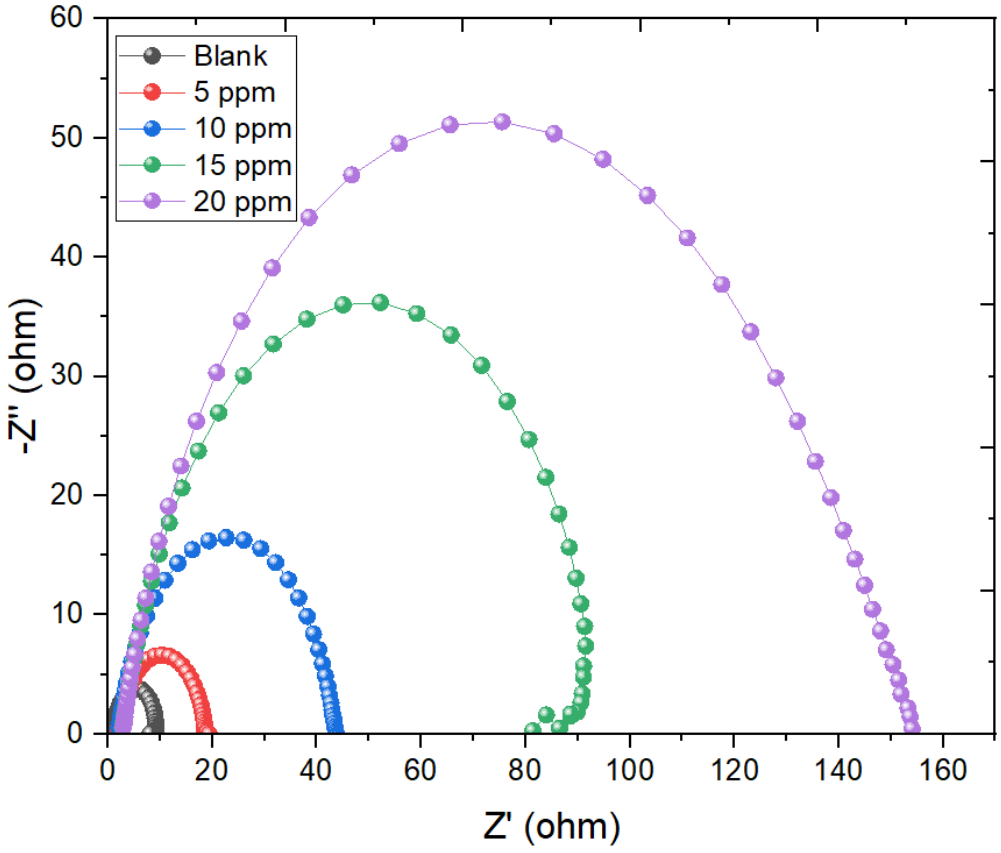
Concentration (ppm)	E_{corr} **(V vs SCE)**	I_{corr} **(A cm^{-2})**	**-βc (V/dec.)**	**βa (V/dec.)**	**Corrosion inhibition efficiency**	**Corrosion rate (mm/year)**
0	-0.490	1.74×10^{-3}	0.08	0.10	0	20.24
5	-0.487	7.23×10^{-4}	0.090	0.068	58.44	5.23
10	-0.477	3.12×10^{-4}	0.094	0.048	82.06	3.82
15	-0.458	2.01×10^{-4}	0.098	0.064	88.44	1.74
20	-0.457	9.80×10^{-5}	0.101	0.064	94.36	0.48

3.5. Electrochemical impedance spectroscopy (EIS) study

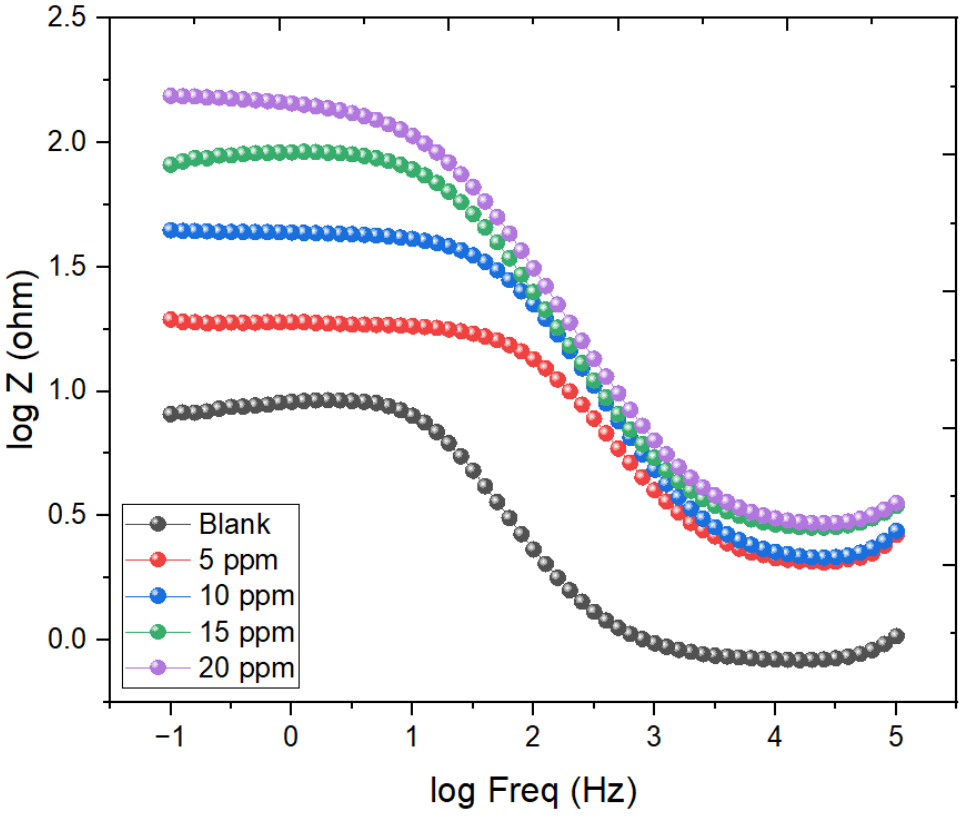
EIS yields essential electrochemical metrics that deliver important information concerning the surface properties of materials subjected to corrosive settings, along with the kinetics related to inhibition mechanisms [23]. The impedance characteristics of steel were evaluated using ANFE as a corrosion inhibitor in varying concentrations of 1 M hydrochloric acid solution. The Nyquist and Bode plots of stainless steel outlined in Figure 2a and 2b respectively has been drawn at different inhibitor concentrations which were acquired in a 1 M HCl solution at 30 °C both in the absence and presence of varying concentrations of ANFE, after 30 minutes of immersion under open-circuit conditions [24]. Table 3 shows a summary of the solution resistance (Rs), charge transfer resistance (R_{ct}), and constant phase element (CPE) that were established from impedance data.

The semicircular profiles as depicted in Nyquist plots (Figure 2a) shows the presence of a single time constant which corresponds to R_{ct}. These semicircular profiles show increase in diameter in addition to inhibitors suggesting a decrease in rate of steel dissipation. This also shows an improvement in inhibitor efficacy.

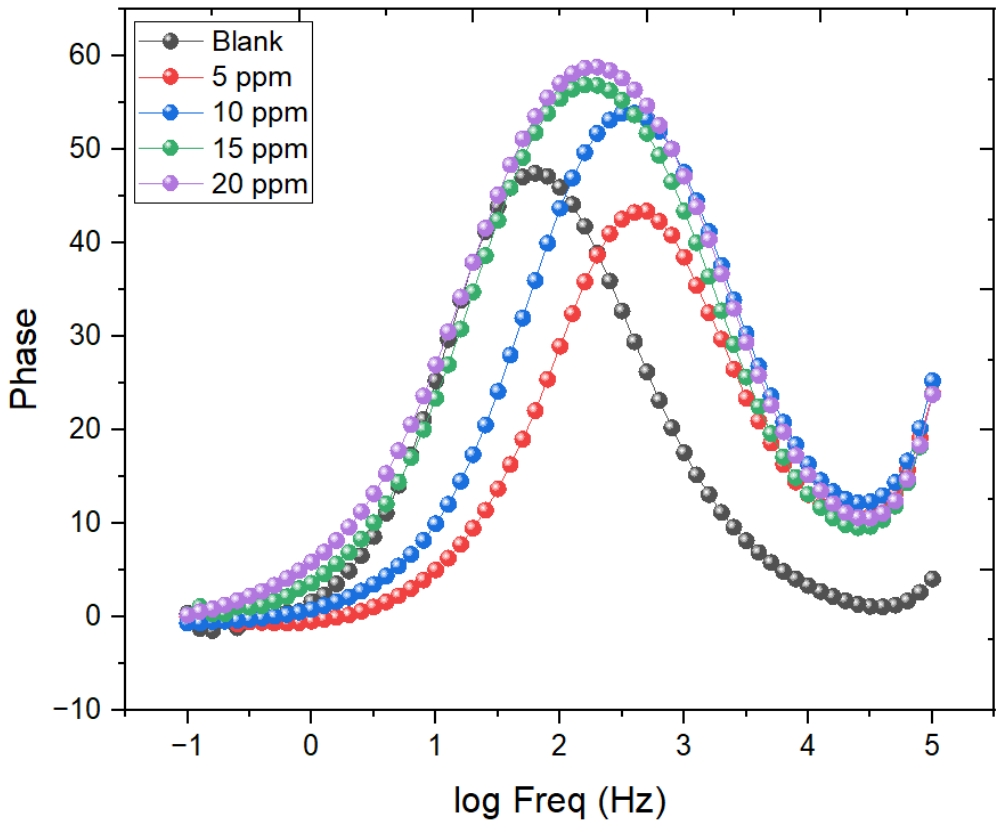
With increasing inhibitor concentration, phase angle in the Bode plots (Figure 2b and 2c) shifts to lower frequencies and significantly widens. This movement demonstrates how a more stable and protective coating gradually forms on the steel's surface [25-28]. The maximum inhibition efficiency of 94.47% at 20 ppm escalates R_{ct} on increasing concentration and also confirms the higher adsorption of phytoconstituents present in ANFE inhibitor, which improves the mild steel resistance to corrosion.



(A)


log Z (ohm)
log Freq (Hz)
Blank
5 ppm
10 ppm
15 ppm
20 ppm
2.5
2.0
1.5
1.0
0.5
0.0
−1
0
1
2
3
4
5

(B)



(C)

Figure 4: Nyquist (A) and, Bode plots (B & C) were generated with and without differing concentrations of ANFE to evaluate its effect on the system impedance properties.

Table 4: Electrochemical Impedance Spectroscopy parameters of stainless steel in 1 M HCl of varying concentrations of ANFE.

Conc. (ppm)	**Rs (*Ω*)**	***R*ct (*Ω*)**	**CPE (*μF*cm^{-2})**	***N***	**Efficiency (%)**
Blank	1.89	7.65	1.65 x10^{-4}	0.84	-
5 ppm	1.90	17.52	7.47 x 10^{-5}	0.83	56.33
10 ppm	1.98	41.89	6.11 x 10^{-5}	0.85	81.73
15 ppm	2.65	95.21	7.83 x 10^{-5}	0.83	87.56

20 ppm	2.72	138.41	6.63×10^{-5}	0.81	**94.47**

4. Conclusion

- ANFE inhibitor used as green and sustainable corrosion inhibitor towards mild steel corrosion in 1 M HCl acidic medium.
- Weight loss measurement and electrochemical analysis exhibited above 90% inhibition efficiency at optimum concentrations and room temperature.
- Surface analysis SEM and EDS reveal the morphology and surface composition of mild steel surface before and after use of inhibitor ANFE.
- Experimental and surface analysis results show good agreements towards corrosion protection on metal surface.

Acknowledgements

Authors would like to thankful to principal Shri Shanakaracharaya Professional University for basic laboratory facility.

Funding Information

The authors declare that this research was conducted without any financial support.

Conflict of interest

Authors declared no conflict of interest.

Consent to Publish declaration

Not applicable.

Ethics and Consent to Participate declarations

Ethical approval and formal permission were not required for this study, as it involved a wild plant species (***Acacia nilotica***) collected from natural habitats. No endangered or protected species were involved, and sampling was conducted responsibly to avoid ecological disturbance. The study complied with standard guidelines for plant research and biodiversity conservation. Plant has been collected from rural area of Rajnandgaon district and stored at public place with Deposition number: PAC/BOT/2026/218. Dr. Trilok Kumar, Asst Professor, Department of

Botany, Govt. Digvijay PG Autonomous College, Rajnandgaon, Chhattisgarh India has been identified and certified the plant.

Authors' contributions

GT-Experiment and Manuscript preparation

MD-Review

BJ-Review

PN-Guidance and Review

AS- Experiment and Manuscript preparation

Data Availability Statement

Yes! Data sharing not applicable to this article as no datasets were generated or analysed during the current study.

Consent to Publish

Not Applicable

References

1. Verma, D. K., & Khan, F. (2016). Corrosion inhibition of mild steel in hydrochloric acid using extract of glycine max leaves. *Research on Chemical Intermediates*, *42*(4), 3489-3506.
2. Miralrio, A., & Espinoza Vázquez, A. (2020). Plant extracts as green corrosion inhibitors for different metal surfaces and corrosive media: a review. *Processes*, *8*(8), 942.
3. Verma, D. K., & Khan, F. (2016). Green approach to corrosion inhibition of mild steel in hydrochloric acid medium using extract of spirogyra algae. *Green chemistry letters and reviews*, *9*(1), 52-60.

4. Peter, A., Obot, I. B., & Sharma, S. K. (2015). Use of natural gums as green corrosion inhibitors: an overview. *International Journal of Industrial Chemistry*, *6*(3), 153-164.
5. Verma, C., Lgaz, H., Verma, D. K., Ebenso, E. E., Bahadur, I., & Quraishi, M. A. (2018). Molecular dynamics and Monte Carlo simulations as powerful tools for study of interfacial adsorption behavior of corrosion inhibitors in aqueous phase: a review. *Journal of Molecular Liquids*, *260*, 99-120.
6. Verma, D. K., Khan, F., Bahadur, I., Salman, M., Quraishi, M. A., Verma, C., & Ebenso, E. E. (2018). Inhibition performance of Glycine max, Cuscuta reflexa and Spirogyra extracts for mild steel dissolution in acidic medium: density functional theory and experimental studies. *Results in Physics*, *10*, 665-674. 6a. International Plant Names Index. Acacia nilotica (L.) Willd. ex Delile., Descr. Egypte, Hist. Nat. 2(Mém.): 79 (1813).
7. Hossain, N., Asaduzzaman Chowdhury, M., & Kchaou, M. (2021). An overview of green corrosion inhibitors for sustainable and environment friendly industrial development. *Journal of Adhesion Science and Technology*, *35*(7), 673-690.
8. Verma, D. K., Ebenso, E. E., Quraishi, M. A., & Verma, C. (2019). Gravimetric, electrochemical surface and density functional theory study of acetohydroxamic and benzohydroxamic acids as corrosion inhibitors for copper in 1 M HCl. *Results in Physics*, *13*, 102194.
9. Verma, D. K., Al Fantazi, A., Verma, C., Khan, F., Asatkar, A., Hussain, C. M., & Ebenso, E. E. (2020). Experimental and computational studies on hydroxamic acids as environmental friendly chelating corrosion inhibitors for mild steel in aqueous acidic medium. *Journal of Molecular Liquids*, *314*, 113651.
10. Verma, C., Verma, D. K., Ebenso, E. E., & Quraishi, M. A. (2018). Sulfur and phosphorus heteroatom-containing compounds as corrosion inhibitors: An overview. *Heteroatom Chemistry*, *29*(4), e21437.
11. Jaiswal, M., Saxena, A., & Kaur, J. (2024). Application of expired Febuxostat drug as an effective corrosion inhibitor for steel in acidic medium: experimental and theoretical studies. *Chemical Data Collections*, *52*, 101149.

12. Raja, P. B., Qureshi, A. K., Rahim, A. A., Osman, H., & Awang, K. (2013). Neolamarckiacadamba alkaloids as eco-friendly corrosion inhibitors for mild steel in 1 M HCl media. Corrosion Science, 69, 292-301.
13. Lgaz, H., Salghi, R., Jodeh, S., &Hammouti, B. (2017). Effect of clozapine on inhibition of mild steel corrosion in 1.0 M HCl medium. *Journal of Molecular Liquids*, *225*, 271-280.
14. Majeed, M. N., Yousif, Q. A., &Bedair, M. A. (2022). Study of the corrosion of nickel–chromium alloy in an acidic solution protected by nickel nanoparticles. *ACS omega*, *7*(34), 29850-29857.
15. Elaryian, H. M., Bedair, M. A., Bedair, A. H., Aboushahba, R. M., & Fouda, A. E. A. S. (2022). Synthesis, characterization of novel coumarin dyes as corrosion inhibitors for mild steel in acidic environment: Experimental, theoretical, and biological studies. *Journal of Molecular Liquids*, *346*, 118310.
16. Hameed, R. A., AlShafey, H. I., & Abu-Nawwas, A. H. (2014). 2-(2, 6-dichloranilino) phenyl acetic acid drugs as eco-friendly corrosion inhibitors for mild steel in 1M HCl. *International Journal of Electrochemical Science*, *9*(11), 6006-6019.
17. Solmaz, R., Kardaş, G. Ü. L. F. E. Z. A., Çulha, M., Yazıcı, B., & Erbil, M. E. H. M. E. T. (2008). Investigation of adsorption and inhibitive effect of 2-mercaptothiazoline on corrosion of mild steel in hydrochloric acid media. *Electrochimica Acta*, *53*(20), 5941-5952.
18. Yadav, D. K., Maiti, B., & Quraishi, M. A. (2010). Electrochemical and quantum chemical studies of 3, 4-dihydropyrimidin-2 (1H)-ones as corrosion inhibitors for mild steel in hydrochloric acid solution. *Corrosion Science*, *52*(11), 3586-3598.
19. Yadav, D. K., & Quraishi, M. A. (2012). Electrochemical investigation of substituted pyranopyrazoles adsorption on mild steel in acid solution. *Industrial & engineering chemistry research*, *51*(24), 8194-8210.
20. Solomon, M. M., Gerengi, H., & Umoren, S. A. (2017). Carboxymethyl cellulose/silver nanoparticles composite: synthesis, characterization and application as a benign corrosion inhibitor for St37 steel in 15% H2SO4 medium. *ACS applied materials & interfaces*, *9*(7), 6376-6389.

21. Bedair, M. A., Soliman, S. A., Bakr, M. F., Gad, E. S., Lgaz, H., Chung, I. M., ... &Alqahtany, F. Z. (2020). Benzidine-based Schiff base compounds for employing as corrosion inhibitors for carbon steel in 1.0 M HCl aqueous media by chemical, electrochemical and computational methods. *Journal of Molecular Liquids*, *317*, 114015.
22. Shoair, A. G. F., Motawea, M. M., Almalki, A. S., Shanab, M. M., El-Basiony, A., &Nasef, H. A. (2024). Expired terazosin as environmentally safe corrosion inhibitor for 1018 carbon steel in 1 M HCl solution: experimental and computational studies. *International Journal of Electrochemical Science*, *19*(1), 100397.
23. Hernández, H. H., Reynoso, A. M. R., Juan, C., González, T., & Morán, C. O. G. (2020). Electrochemical Impedance Spectroscopy (EIS): A Review Study of Basic Aspects of the Corrosion Mechanism Applied to. *Electrochemical impedance spectroscopy*, 1.
24. Touhami, F., Aouniti, A., Abed, Y., Hammouti, B., Kertit, S., Ramdani, A., &Elkacemi, K. (2000). Corrosion inhibition of armco iron in 1 M HCl media by new bipyrazolic derivatives. *Corrosion science*, *42*(6), 929-940.
25. Dohare, P., Chauhan, D. S., Sorour, A. A., & Quraishi, M. A. (2017). DFT and experimental studies on the inhibition potentials of expired Tramadol drug on mild steel corrosion in hydrochloric acid. *Materials discovery*, *9*, 30-41.
26. Elebo, A., Uba, S., Ekwumemgbo, P. A., & Ajibola, V. O. (2024). Unravelling adsorption potential of expired clindamycin as corrosion inhibitor at mild Steel/HCl interface via response surface methodology, artificial neural network, electrochemical, and computational strategies. *Current Research in Green and Sustainable Chemistry*, *8*, 100402.
27. Verma, D. K., Kaya, S., Ech-Chihbi, E., El-Hajjaji, F., Phukan, M. M., & Alnashiri, H. M. (2021). Investigations on some coumarin based corrosion inhibitors for mild steel in aqueous acidic medium: electrochemical, surface morphological, density functional theory and Monte Carlo simulation approach. *Journal of Molecular Liquids*, *329*, 115531.
28. Haldhar, R., Prasad, D., Bahadur, I., Dagdag, O., Kaya, S., Verma, D. K., & Kim, S. C. (2021). Investigation of plant waste as a renewable biomass source to develop efficient, economical and eco-friendly corrosion inhibitor. *Journal of Molecular Liquids*, *335*, 116184.

Supplementary Files

This is a list of supplementary files associated with this preprint. Click to download.

- 31.3.26Acacianilotica.pdf
- AcaciaNiloticadentification.pdf